This is a repository copy of *The latitudinal diversity gradient of tetrapods across the Permo-Triassic mass extinction and recovery interval*.

White Rose Research Online URL for this paper:
http://eprints.whiterose.ac.uk/161099/

Version: Accepted Version

Title: The latitudinal diversity gradient of tetrapods across the Permo-Triassic mass extinction and recovery interval

Authors: Bethany J. Allen[1]*, Paul B. Wignall[1], Daniel J. Hill[1], Erin E. Saupe[2] and Alexander M. Dunhill[1]

[1] School of Earth and Environment, University of Leeds, Leeds, UK

[2] Department of Earth Sciences, University of Oxford, Oxford, UK

* Corresponding author: eebja@leeds.ac.uk

Abstract:

The decline in species richness from the equator to the poles is referred to as the latitudinal diversity gradient (LDG). Higher equatorial diversity has been recognised for over 200 years, but the consistency of this pattern in deep time remains uncertain. Examination of spatial biodiversity patterns in the past across different global climate regimes and continental configurations can reveal how LDGs have varied over Earth history and potentially differentiate between suggested causal mechanisms. The Late Permian–Middle Triassic represents an ideal time interval for study, because it is characterised by large-scale volcanic episodes, extreme greenhouse temperatures, and the most severe mass extinction event in Earth history. We examined terrestrial and marine tetrapod spatial biodiversity patterns using a database of global tetrapod occurrences. Terrestrial tetrapods exhibit a bimodal richness distribution throughout the Late Permian–Middle Triassic, with peaks in the northern low latitudes and southern mid latitudes around 20-40°N and 60°S, respectively. Marine reptile fossils are known almost exclusively from the Northern Hemisphere in the Early and Middle Triassic, with highest diversity around 20°N. Reconstructed LDGs contrast strongly with the generally unimodal terrestrial gradients of today, potentially reflecting high global temperatures and prevailing Pangean super-monsoonal climate system during the Permo-Triassic.

1 Background

2 The latitudinal diversity gradient (LDG) is one of the largest-scale and longest-known

3 patterns in ecology [e.g.1-7]. Modern biodiversity (i.e., richness) gradients are broadly

4 defined as unimodal, with high biodiversity near the equator and low biodiversity at the poles

5 [4,6]. The specifics of these gradients differ among taxonomic and ecological groups [2-4,6],

6 and research over the last decade has revealed greater variation in modern LDGs than

7 previously recognised. For example, benthic marine species richness appears to peak at 10-

8 20°N, whereas pelagic species richness appears bimodal, with peaks at 10-40° on either

9 side of the equator [8-11].

10 Study of the fossil record suggests the shape of LDGs has also changed through time

11 [5,12]. Dinosaur diversity may have been greatest at temperate latitudes throughout the

12 Mesozoic [13], North American mammal diversity may have been distributed evenly across

13 latitudes for much of the Cenozoic [14,15], and peaks in marine animal diversity may have

14 drifted from the Southern to Northern Hemisphere over the course of the Phanerozoic

15 [16,17].

16 Numerous drivers of LDGs have been proposed [e.g.2,3,18-22]. Interaction between key

17 processes, the complexity of feedback cycles, and the covariance of many environmental

18 variables with latitude complicate efforts to isolate causal mechanisms [2-4,6,23]. Climate

19 and landmass distribution, however, have been put forward consistently as potential

20 explanatory variables. Climate, particularly temperature and water availability, has long been

21 considered a key control on spatial patterns of terrestrial biodiversity [5,12,14,15,17,24-26]

22 because the distributions of species are limited by climatic tolerance [22,24,27-30].

23 LDG studies in deep time have suggested palaeoclimate regime is a major control on the

24 shape and slope of LDGs. Icehouse periods have been associated with a sharp, unimodal

25 equatorial richness peak, and greenhouse periods with a bimodal distribution, characterised

26 by shallow peaks at mid-latitudes of both the Northern and Southern Hemispheres [5,17,31].

27 This contrast has been attributed to the strength of the pole-to-equator temperature gradient

28 between the two climate regimes [5,13,17], but may also reflect spatio-temporal variations in

29 precipitation [14,22,25]. The distribution of continental landmasses may also structure global

30 patterns of biodiversity by controlling the spatial distribution of relevant habitats, particularly

31 shallow continental shelf area in marine ecosystems [32-35]. Although studies of modern

32 LDGs continue to provide insight into potential generative mechanisms [e.g.36-39],

33 examination of LDGs during intervals when climate and landmass distribution were

34 considerably different to today may provide new perspectives on global biodiversity patterns

35 and their associated processes [5,13,31].

36   The Late Permian to Middle Triassic (~260-239 Ma) represents a period in Earth history
37   that contrasts considerably with the present day. Large-scale volcanism associated with the
38   Siberian Traps drove extreme climate change, which was exacerbated by amalgamation of
39   most landmasses into the supercontinent Pangea [40-42]. This drove environmental
40   perturbations that resulted in the most catastrophic mass extinction event of all time at the
41   end of the Permian, around 252 Ma [43]. A prolonged interval of extremely high
42   temperatures, which peaked in the Olenekian (late Early Triassic) [44], along with ocean
43   anoxia and acidification have been identified as key extinction mechanisms [43,45], with
44   persistence of these conditions extending well into the Middle Triassic, delaying full
45   structural recovery of marine ecosystems for as long as 50 million years [46]. On land, high
46   temperatures and seasonal precipitation in central Pangaea resulted in drought [40,47-49],
47   while purported ozone depletion, brought about by halogen gas release from the Siberian
48   Traps, resulted in high UV-B levels that caused plant sterilisation and extinction [e.g.50,51].
49   Early Triassic temperatures at low latitudes are considered to have been beyond the
50   tolerable long-term threshold for both plants and animals, driving extinction and poleward
51   migration [44,52]. The climate of the Middle Triassic has received less attention, but is
52   thought to have been characterised by continued aridity in lower latitudes, with cyclical
53   temperature fluctuations overprinting a general trend of steady cooling after the final
54   eruptions of the Siberian Traps in the Olenekian [41,42].

55   Tetrapods were profoundly affected by the Permo-Triassic mass extinction (PTME). In
56   the immediate aftermath, Early Triassic tetrapod communities were composed almost
57   entirely of 'disaster fauna' such as Lystrosaurus, a herbivorous burrowing synapsid [47,53-
58   55]. Following recovery from the PTME, archosauromorphs (Sauria), a group that appeared
59   in the Middle Permian, became the dominant terrestrial animals [55]. The first marine reptile
60   fossils are known from the Olenekian and were highly diverse by the Anisian, including basal
61   sauropterygians and ichthyosaurs [56].

62   Two previous studies have offered perspectives on the distribution of tetrapods across
63   the Permo-Triassic boundary. Sun et al. [44] used oxygen isotopes in conodont apatite to
64   examine sea surface temperature (SST) change across the Late Permian and Early Triassic,
65   recovering remarkably high SSTs throughout the interval but particularly during the
66   Smithian–Spathian Thermal Maximum (~248 Ma), when equatorial SSTs may have
67   approached 40°C. Their qualitative analysis of tetrapod occurrences revealed an equatorial
68   'tetrapod gap' in the Early Triassic, hypothesised to have occurred due to the extreme warm
69   temperatures that may have approached or exceeded the thermal tolerances of both
70   terrestrial and marine vertebrates (around 42°C [57]). Bernardi et al. [52] also examined the
71   distribution of individual tetrapod skeletal and footprint occurrences through the extinction

72 and recovery interval, finding evidence for a poleward shift in tetrapod abundance in the
73 Northern Hemisphere, but only in the Induan (earliest Triassic). This biogeographic pattern is
74 congruent with a study of tetrapods immediately prior to the PTME, which found higher
75 tetrapod diversity at temperate than equatorial latitudes during the Middle – Late Permian
76 [58].

77 Here, we explore further the terrestrial and marine Permo-Triassic fossil tetrapod record
78 by comparing species-level tetrapod biodiversity across latitudinal bins. We apply coverage-
79 based interpolation and squares extrapolation to reconstruct LDGs from the Late Permian
80 (before the PTME), Early Triassic (in the aftermath of the PTME) and Middle Triassic (during
81 recovery). These LDGs are then assessed in light of the hypothesis that higher diversity will
82 be found in the cooler refugia of the mid to high latitudes during extreme greenhouse
83 conditions, such as during the Late Permian to Middle Triassic.

84

Methods

86 We conducted an in-depth literature review to maximise the completeness and robustness of
87 our Late Permian to Late Triassic dataset for tetrapods. All tetrapod fossils from the
88 Wuchiapingian (early Late Permian) through Carnian (early Late Triassic) were downloaded
89 from the Paleobiology Database (PBDB). Genus names from this download were used to
90 conduct a systematic literature search in Google Scholar, and any new taxa and
91 occurrences were added to the PBDB. Once completed, the same criteria were used to
92 download the enlarged dataset (in October 2018) [59]. We reviewed each 'collection',
93 representing fossils from a particular locality and considered to be of a similar age, to
94 increase temporal resolution. A literature search for formation names was conducted, with
95 publications that listed the ages of specific beds or members further refining the geological
96 date of collections, where possible [59]. We streamlined the mode of preservation and taxon
97 habitat categories, reduced to either 'body' or 'trace', and 'marine' or 'terrestrial',
98 respectively. Finally, the modern latitude and longitude of fossil localities were rotated to
99 their palaeo-position at the time of deposition by filtering occurrences on a stage-by-stage
100 basis then using the PALEOMAP Global Plate Model [60], implemented in G-Plates (version
101 2.1.0) [61]. The final dataset constituted 3563 unique tetrapod occurrences assigned to
102 stage level, with our search efforts contributing 490 of these occurrences (13.8%).

103 All subsequent data manipulation and plotting was carried out in R [62] utilising the
104 'tidyverse' suite of packages [63]. The final dataset was filtered to include only records
105 representing unique species, comprising those identified to species level and those identified
106 to coarser taxonomic levels but representing a clade not already within their spatiotemporal

107   bin. Since abundance data in the Paleobiology Database are relatively incomplete and
108   inconsistently applied, the presence of a species within any given collection was treated as a
109   single occurrence. Fossil occurrences dated to a single geological stage were used to
110   produce raw sampled-in-bin tetrapod richness curves.

111   To compare tetrapod richness patterns across space between the Late Permian, Early
112   Triassic, and Middle Triassic, stage-level occurrences were binned using 20° latitudinal
113   bands, from 90°S to 90°N (the central bin includes the equator, from 10°N t o 10°S).
114   Terrestrial and marine body fossils were analysed separately, with 'marine tetrapods'
115   referring to species whose morphology indicates life in marine habitats. This informal group
116   is polyphyletic and includes basal ichthyosaurs, sauropterygians, tanystropheids and
117   thalattosaurs.

118   When reconstructing historical spatial biodiversity patterns, allowances must be made for
119   the spatiotemporal unevenness of the fossil record [5,56,64-70]. LDGs in deep time can be
120   estimated if sampling rates in the clade of interest are relatively high, and consideration is
121   given to partitioning variation in richness likely attributable to sampling biases versus that
122   likely attributable to biological patterns [71]. Furthermore, subsampling and extrapolation
123   methods can help alleviate issues of sampling heterogeneity. Coverage-based approaches
124   are currently the most effective approach for mitigating the effects of fossil record bias in
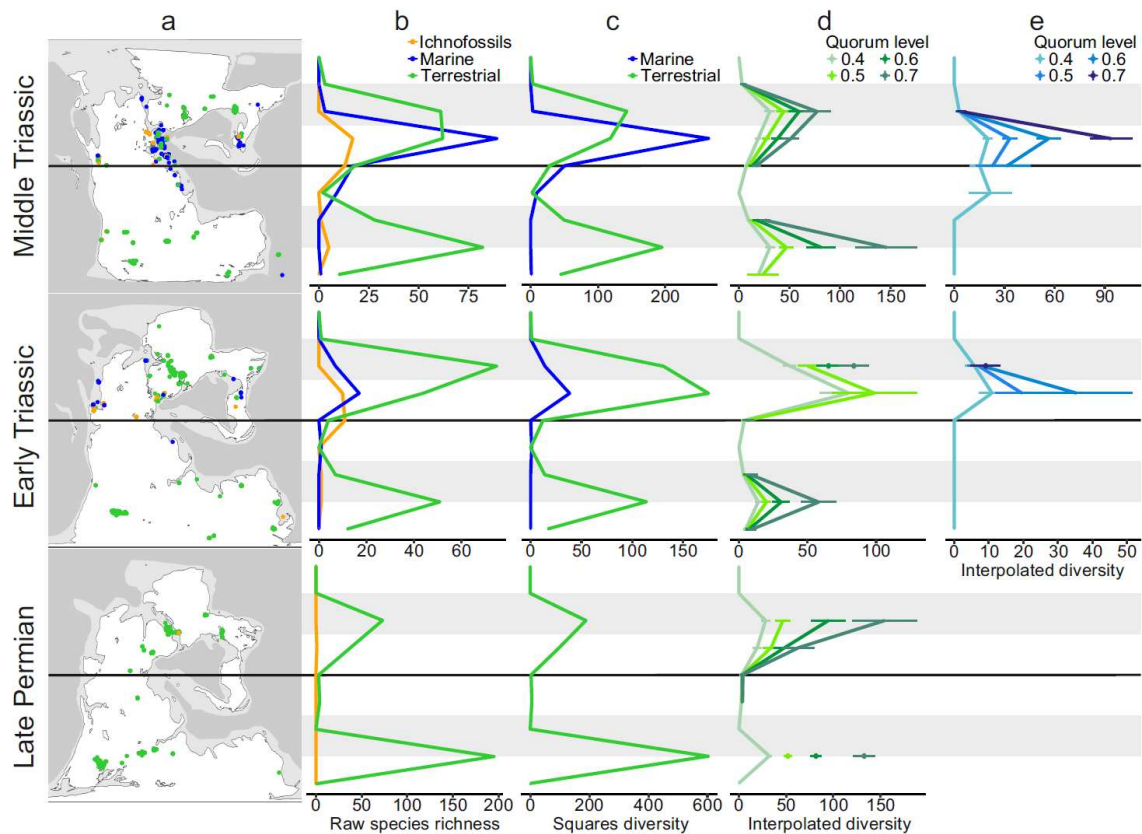125   large-scale biodiversity analyses [72,73].

126   We applied two analytical approaches to account for spatiotemporal sampling biases
127   in occurrence data: coverage-based interpolation [74,75] and squares [76]. Both were
128   applied to collections within latitudinal bins for the Late Permian, Early Triassic, and Middle
129   Triassic time intervals (analyses were repeated for individual stages, Figure S2). Only body
130   fossils were used for these analyses, due to the biological non-equivalence of trace fossil
131   and body fossil species; one animal can produce multiple trace fossils, and traces are not
132   easily allied to individual body fossil species.

133   Richness estimates were generated using coverage-based interpolation following the
134   approach of Dunne et al. [77] using the R package iNEXT [75]. This approach conducts
135   coverage-based rarefaction using the equations of Chao & Jost [74] (analogous to
136   shareholder quorum subsampling [64,72]) and extrapolation based on the Chao1 estimator.
137   Extrapolated estimates were discarded if more than three times the observed sample size,
138   as this suggests a high species-to-occurrence count ratio that indicates the bin under
139   consideration is likely to be undersampled [75]. Bins containing fewer than three species
140   were incompatible with subsampling and therefore excluded from analyses (Table S1).
141   Coverage-based rarefaction curves are also presented (Figure S3) to illustrate the

142   relationship between coverage and coverage-standardised diversity estimates in each bin

143   [72,77].

144   In addition to coverage-based interpolation, richness estimates were generated using

145   the squares method [76]. Squares is an extrapolater based on the proportion of singletons in

146   a given sample, and is considered more robust to biases arising from small sample sizes

147   and uneven abundance distributions than other interpolation methods [73,76]. Squares

148   richness estimates were produced using the equation stated by Alroy [76].

149   Finally, we tested whether variation in sampling intensity among time bins influenced

150   richness estimates, particularly given the expected reduction in Early Triassic tetrapod

151   occurrences following the PTME. We subsampled to the same number of collections in each

152   time interval (Late Permian, Early Triassic and Middle Triassic) using a bootstrap routine.

153   For each time bin, we randomly sampled 250 collections for terrestrial tetrapods and 30

154   collections for marine tetrapods. Collections were allocated to their corresponding latitudinal

155   bin and species richness was quantified across collections within each bin. This process was

156   repeated 100 times. Diversity curves were produced using the mean species diversity in

157   each latitude bin across the 100 replicates, allowing for comparison of LDGs among time

158   bins given an artificially-fixed sampling intensity.

159

Figure 1

Tetrapod diversity by latitude in the Late Permian, Early Triassic and Middle Triassic. The grey bars indicate 30-60°N and S.

a. Palaeo-rotated occurrence locations plotted over maps from Scotese [59]; maps represent the Lopingian, Induan-Olenekian, and Ladinian.

b. Raw occurrences within 20° latitude bins (e.g. central bin is 10°N-10°S).

c. Squares diversity by latitudinal bin for terrestrial (green) and marine (blue) tetrapods.

d. Interpolated diversity by latitudinal bin for terrestrial tetrapods. Bins with < 3 species have been plotted as '0', while missing points indicate an estimated diversity of more than three times the observed value. Error bars indicate 95% confidence intervals.

e. Interpolated diversity by latitudinal bin for marine tetrapods. Bins with < 3 species have been plotted as '0', while missing points indicate an estimated diversity of more than three times the observed value. Error bars indicate 95% confidence intervals. The oldest marine tetrapod fossils are Olenekian (late Early Triassic; 251-247Ma) in age.

174 **Results**

175 Sampling

176 Raw richness, squares and interpolation estimates produced similar diversity-through-time

177 curves (Figure S1). The number of collections with terrestrial tetrapod body fossils was

178 relatively consistent through time (Late Permian, 291; Early Triassic, 307; Middle Triassic,

179 354), while the number of collections containing marine tetrapods increased from the Early

180 to Middle Triassic (Early Triassic, 32; Middle Triassic, 207). Curves of raw species richness

181 by latitude bin produced by bootstrapping to the same number of collections for each time

182 interval were near-identical to those using the full datatset (Figure S4).

183 Terrestrial distribution

184 Terrestrial tetrapod occurrences were broadly distributed but clustered throughout the

185 studied interval (Figure 1a). Both squares and interpolation analyses of terrestrial tetrapods

186 by latitude (Figure 1c) show a consistent bimodal richness distribution throughout the Late

187 Permian to Middle Triassic, with a persistent dip in diversity in the low southern latitudes. In

188 the Northern Hemisphere, diversity peaked at 40°N in the Late Permian. By the Early

189 Triassic, the peak in species diversity had shifted to the 20°N bin (Figure 1b), with stage-

190 level analyses indicating this occurred in the Olenekian (Figure S2b). In the Middle Triassic,

191 the Northern Hemisphere peak returned to 40°N. The gradient in the Southern Hemisphere

192 remained relatively unchanged throughout the Late Permian to Middle Triassic,

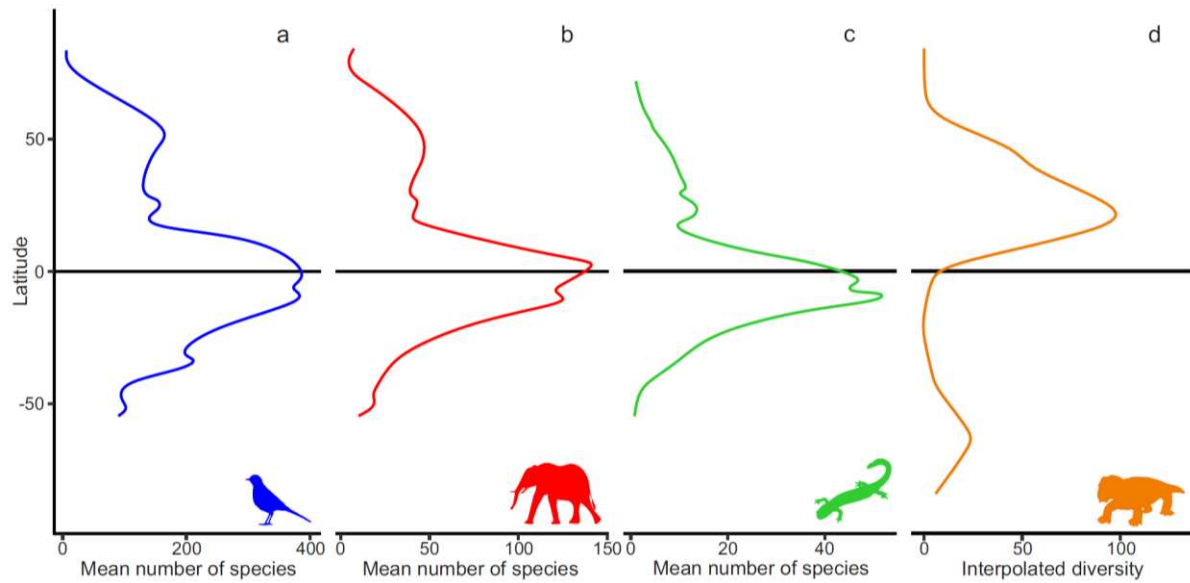193 characterised by a consistent 60°S diversity peak.

194 Marine distribution

195 Marine tetrapods were generally restricted to the Northern Hemisphere during the Early

196 and Middle Triassic, despite having a relatively broad longitudinal distribution (Figure 1a).

197 Early Triassic marine tetrapods were most diverse in the 20°N bin, with the only other

198 occurrences found in the 40°N bin (Figure 1d). The 20°N peak in biodiversity persisted into

199 the Middle Triassic, but with new occupation of the equatorial and 20°S bins. The stage-level

200 analyses generally show comparable trends to those seen in the epoch-level time bins, but

201 often with fewer bins occupied, producing patchier and less constrained gradients (Figure

202 S2).

203 Comparison with modern LDGs

204 The Early Triassic terrestrial LDG produced by interpolation was compared to LDGs of

205 modern birds, mammals and amphibians (Figure 2; modern data derived from

206 BiodiversityMapping.org, as used by Saupe et al. [22]). The modern curves have unimodal

207   distributions that peak at low latitudes (maximum diversity at 9.5°S for birds and amphibians,
208   2.5°N for mammals), whereas the Early Triassic terrestrial curve peaks at higher latitudes ,
209   with a clear bimodal distribution (maximum diversity at 32.5°N and 62.5° S).

210

Figure 2

Smoothed latitudinal gradients for species of modern birds (a), mammals (b), and
amphibians (c), compared with Early Triassic terrestrial tetrapods (as an example) based on
interpolation analyses (d). Modern gradients derive from data obtained from
BiodiversityMapping.org. Silhouettes are from Phylopic.org.

Discussion

In contrast to gradients for modern terrestrial tetrapods, the Permo-Triassic terrestrial tetrapod gradient was likely bimodal with reduced diversity at low latitudes (10°N-30°S) (Figure 1) [4,6]. The general shape of the terrestrial tetrapod richness gradient, particularly its bimodality, remained relatively constant throughout the Late Permian to Middle Triassic, and may reflect the prevailing climate regime (greenhouse versus icehouse) [5,17,31]. Interestingly, the shape of the gradient did not seem affected by the PTME or even higher temperatures of the Early Triassic (equatorial SSTs increased from ~24°C in the latest Permian to ~40°C during the late Smithian [44]). Marine tetrapods, by contrast , maintained a diversity peak at low latitudes in the Northern Hemisphere from the Early to Middle Triassic (Figure 1). The bimodal terrestrial LDG obtained here is comparable to the distribution of raw Early Triassic tetrapod occurrences from Sun et al. [44] and Bernardi et al. [52], and suggests continuity of LDG shape from the Middle Permian [58]. The shape of the gradient is also broadly comparable to the gradient of Mesozoic dinosaurs, which Mannion et al. [13] attributed to the distribution of land area during the break-up of Pangaea. This congruence suggests LDGs may have been bimodal for much of the Permian to mid Cenozoic, with modern LDGs only developing as global climate gradually cooled through the late Paleogene and early Neogene [5,14,15,31].

Although latitude is a reasonable proxy for temperature in the modern, this relationship does not hold for the Triassic [41]. The latitudinal temperature gradient today largely reflects the operation of Hadley cells, but these cells may have collapsed in the Late Permian to give way to a more zonally asymmetric atmospheric system, with strong seasonal variation in temperature and precipitation [40,41,49]. Although the Tethyan coastal regions experienced supermoonsoons, considerably less precipitation reached the continental interior, resulting in high aridity, particularly in the southern low to mid latitudes [40,43]. Climate model reconstructions for the latest Permian suggest large areas of central Pangea were desert, with seasonal average temperatures up to 45°C in the arid subtropics at 20-25°N and S [78]. Late Permian palaeoenvironmental evidence from localities in South Africa indicates considerable drought even at relatively high latitudes (~65°S) [47]. Thus, much of the supercontinent interior may have been uninhabitable in the Late Permian, which could explain the bimodal, asymmetric tetrapod LDG reconstructed here. However, in contrast to Permian climates, Triassic climates have not been well studied [41,42], and the development of high-resolution climate models for the Triassic is essential for determining the key drivers of tetrapod extinction and migration during this interval.

250   We cautiously interpret the bimodal richness distributions found here as biologically
251   meaningful, particularly given the agreement between the different sampling methodologies
252   employed. In addition, collections from southern low latitude regions are consistently of low
253   alpha diversity throughout the entire Late Permian to Middle Triassic, in comparison with
254   some very high levels of alpha diversity in mid-latitude collections during the same intervals
255   (Table S2). However, the spatial and temporal resolution of the analyses, and our certainty
256   in the observed distributions representing biological patterns, would benefit from better
257   geographic spread and higher density of samples [67-69]. New discoveries from the
258   southern low to mid latitudes could particularly help to distinguish between low biodiversity
259   and poor sampling, but fossiliferous outcrops of this age and palaeolatitude are uncommon,
260   particularly from terrestrial environments (Figure S5) [41,49,67]. Although extensive shallow
261   and marginal marine deposits, such as those in Oman, are rich in invertebrate fossils
262   [e.g.79], vertebrate fossils are known only from a handful of localities, such as Gour Laoud in
263   Algeria (Jesairosaurus lehmani, Odenwaldia sp., indeterminate amphibians; palaeolatitude
264   9°S [80]) and Mariakani in Kenya (Kenyasaurus mariakaniensis; palaeolatitude 42°S [81]).
265   Unfortunately, the age of fossils from these localities is poorly constrained and were
266   therefore not included in our analyses.

267   Although broad stasis in bimodal richness gradients was observed over the ~23
268   million year interval considered here (Late Permian – Middle Triassic), smaller-scale
269   variability can be detected among time bins. Both squares and interpolation analyses
270   suggest a shift in peak diversity in the Northern Hemisphere towards the equator in the Early
271   Triassic, before returning to mid-latitudes in the Middle Triassic. This shift is also supported
272   by the relatively high number of trace fossil occurrences in the equatorial and 20°N bins
273   during the Early Triassic (Figure 1b). An Early Triassic equatorward shift in diversity in the
274   Northern Hemisphere seems surprising given that global temperatures were increasing at
275   the time [44]. Instead, this shift may reflect differential sampling bias. Most of the
276   interpolation rarefaction curves are exponential in shape, but the Early Triassic 20°N bin has
277   a more asymptotic curve (Figure S3), indicating sampling completeness may be substantially
278   higher in this bin relative to the others, inflating diversity estimates [72]. This peak in diversity
279   corresponds to the high density of tetrapod fossils known from the Olenekian of Eastern
280   Europe [82].

Conclusions

Our results suggest terrestrial tetrapods exhibited a bimodal richness distribution and were most diverse at mid-latitudes during the Late Permian – Middle Triassic. In contrast, marine tetrapods were generally restricted to northern low latitudes in the Early and Middle Triassic. Tetrapods were not excluded from equatorial regions during this interval, but were reduced in diversity at low southern latitudes. The bimodal LDG for terrestrial tetrapods during the Late Permian – Middle Triassic contrasts with the unimodal, equatorial diversity peaks exhibited by most terrestrial tetrapod clades in the modern, including birds, mammals and amphibians (Figure 2). Permo-Triassic LDGs were likely shaped by the extreme climatic conditions of the time, particularly high global temperatures and heterogeneous precipitation. As is often the case regarding the vertebrate fossil record, our data are insufficient to determine conclusively whether observed patterns predominantly reflect true biological signal or heterogeneous spatial sampling. Further examination of Triassic climates and increased sampling intensity may advance our understanding of this time interval, providing greater insight into the potential influence of extreme greenhouse conditions on global patterns of biodiversity.

330   **References**

331   1. von Humboldt A, Bonpland A. 2009 [1807] Essay on the geography of plants. In:
332   Jackson ST, editor. Romanowski S, translator. Essay on the Geography of Plants.
333   University of Chicago Press. p49-144.

334   2. Gaston KJ. 2000 Global patterns in biodiversity. Nature **405**, 220-227.
335   (doi:10.1038/35012228)

336   3. Willig MR, Kaufman DM, Stevens RD. 2003 Latitudinal gradients of biodiversity:
337   pattern, process, scale and synthesis. Annu. Rev. Ecol. Evol. Syst. **34**, 273-309.
338   (doi:10.1146/annurev.ecolsys.34.012103.144032)

339   4. Hillebrand H. 2004 On the generality of the latitudinal diversity gradient. Am. Nat.
340   **163**, 192-211. (doi:10.1086/381004)

341   5. Mannion PD, Upchurch P, Benson RBJ, Goswami A. 2014 The latitudinal diversity
342   gradient through deep time. TREE **29**, 42-50. (doi:10.1016/j.tree.2013.09.012)

343   6. Kinlock NL, Prowant L, Herstoff EM, Foley CM, Akin-Fajiye M, Bender N, Umarani M,
344   Yeong Ryu H, Şen B, Gurevitch J. 2018 Explaining global variation in the latitudinal
345   diversity gradient: meta-analysis confirms known patterns and uncovers new ones.
346   Global Eco. Biogeog. **27**, 125-141. (doi:101111/geb.12665)

347   7. Saupe EE, Farnsworth A, Lunt DJ, Sagoo N, Pham KV, Field DJ. 2019a Climatic
348   shifts drove major contractions in avian latitudinal distributions throughout the
349   Cenozoic. PNAS **116**, 12895-12900. (doi: 10.1073/pnas.1903866116)

350   8. Tittensor DP, Mora C, Jetz W, Lotze HK, Ricard D, Vanden Berghe E, Worm B. 2010
351   Global patterns and predictors of marine biodiversity across taxa. Nature **466**, 1098-
352   1101. (doi:10.1038/nature09329)

353   9. Powell MG, Beresford VP, Colaianne BA. 2012 The latitudinal position of peak
354   marine diversity in living and fossil biotas. J. Biogeogr. **39**, 1687-1694.
355   (doi:10.1111/j.1365-2699.2012.02719.x)

356   10. Chaudhary C, Saeedi H, Costello MJ. 2016 Bimodality of latitudinal diversity
357   gradients in marine species richness. TREE **31**, 670-676.
358   (doi:10.1016/j.tree.2016.06.001)

359   11. Chaudhary C, Saeedi H, Costello MJ. 2017 Marine species richness is bimodal with
360   latitude: a reply to Fernandez and Marques. TREE **32**, 234-237.
361   (doi:10.1016/j.tree.2017.02.007)

362   12. Crame JA. 2001 Taxonomic diversity gradients through geological time. Divers.
363   Distrib. **7**, 175-189. (doi: 10.1111/j.1472-4642.2001.00106.x)

364   13. Mannion PD, Benson RBJ, Upchurch P, Butler RJ, Carrano MT, Barrett PM. 2012 A
365   temperate palaeodiversity peak in Mesozoic dinosaurs and evidence for Late

366   Cretaceous geographical partitioning. Global Eco. Biogeog. **21**, 898-908.

367   (doi:10.1111/j.1466-8238.2011.00735.x)

368   14. Fraser D, Hassall C, Gorelick R, Rybczynski N. 2014 Mean annual precipitation

369   explains spatiotemporal patterns of Cenozoic mammal beta diversity and latitudinal

370   diversity gradients in North America. PLoS One **9**, e106499.

371   (doi:10.1371/journal.pone.0106499)

372   15. Marcot JD, Fox DL, Niebuhr SR. 2016 Late Cenozoic onset of the latitudinal diversity

373   gradient of North American mammals. PNAS **113**, 7189-7194.

374   (doi:10.1073/pnas.1524750113)

375   16. Powell MG. 2009 The latitudinal diversity gradient of brachiopods over the past 530

376   million years. Jour. Geol. **117**, 585-594. (doi:10.1086/605777)

377   17. Naimark EB, Markov AV. 2011 Northward shift in faunal diversity: a general pattern

378   of evolution of Phanerozoic marine biota. Biol. Bull. Rev. **1**, 71-81.

379   18. Clarke A, Gaston KJ. 2006 Climate, energy and diversity. Proc. R. Soc. B **273**, 2257-

380   2266. (doi:10.1098/rspb.2006.3545)

381   19. Mittelbach GG, Schemske DW, Cornell HV, Allen AP, Brown JM, Bush MB, Harrison

382   SP, Hurlbert AH, Knowlton N, Lessios HA et al. 2007 Evolution and the latitudinal

383   diversity gradient: speciation, extinction and biogeography. Ecol. Lett. **10**: 315-331.

384   (doi: 10.1111/j.1461-0248.2007.01020.x)

385   20. Schemske DW, Mittelbach GG, Cornell HV, Sobel JM, Roy K. 2009 Is there a

386   latitudinal diversity gradient in the importance of biotic interactions? Annu. Rev. Ecol.

387   Evol. Syst. **40**, 245-269. (doi: 10.1146/annurev.ecolsys.39.110707.173430)

388   21. Archibald SB, Bossert WH, Greenwood DR, Farrell BD. 2010 Seasonality, the

389   latitudinal gradient of diversity, and Eocene insects. Paleobiology **36**, 374-398. (doi:

390   10.1666/09021.1)

391   22. Saupe EE, Myers CE, Peterson AT, Soberón J, Singarayer J, Valdes P, Qiao H.

392   2019b Spatio-temporal climate change contributes to latitudinal diversity gradients.

393   Nature Ecol. Evol. In press. (doi: 10.1038/s41559-019-0962-7)

394   23. Jablonski D. 2008 Extinction and the spatial dynamics of biodiversity. PNAS **105**,

395   11528-11535. (doi:10.1073/pnas.0801919105)

396   24. Brown JH. 1984 On the relationship between abundance and distribution of species.

397   Am. Nat. **124**, 255-279. (doi:10.1086/284267)

398   25. Hawkins BA, Field R, Cornell HV, Currie DJ, Guégan J-F, Kaufman DM, Kerr JT,

399   Mittelbach GG, Oberdorff T, O'Brien EM et al. 2003 Energy, water, and broad-scale

400   geographic patterns of species richness. Ecology **84**, 3105-3117. (doi:10.1890/03-

401   8006)

26. Currie DJ, Mittelbach GG, Cornell HV, Field R, Guégan J-F, Hawkins BA, Kaufman DM, Kerr JT, Oberdorff T, O'Brien E et al. 2004 Predictions and tests of climate-based hypotheses of broad-scale variation in taxonomic richness. Ecol. Lett. **7**, 1121-1134. (doi:10.1111/j.1461-0248.2004.00671.x)

27. Grinnell J. 1917 The niche-relationships of the California Thrasher. The Auk **34**, 427-433. (doi:10.2307/4072271)

28. Hutchinson GE. 1957 Concluding remarks. Cold Spring Harbour Symp. Quant. Biol. **22**, 415-427.

29. Root T. 1988 Energy constraints on avian distributions and abundances. Ecology **69**, 330-339.

30. Powell MG. 2007 Geographic range and genus longevity of late Paleozoic brachiopods. Paleobiology **33**, 530-546. (doi: 10.1666/07011.1)

31. Meseguer AS, Condamine FL. 2020 Ancient tropical extinctions at high latitudes contributed to the latitudinal diversity gradient. Evolution in press. (doi:10.1111/evo.13967)

32. Valentine JW, Moores EM. 1970 Plate-tectonic regulation of faunal diversity and sea level: a model. Nature **228**, 657-659.

33. Mannion PD, Benson RBJ, Carrano MT, Tennant JP, Judd J, Butler RJ. 2015 Climate constrains the evolutionary history and biodiversity of crocodylians. Nat. Commun. **6**, 8438. (doi:10.1038/ncomms9438)

34. Vavrek MJ. 2016 The fragmentation of Pangaea and Mesozoic terrestrial vertebrate biodiversity. Biol. Lett. **12**, 20160528. (doi:10.1098/rsbl.2016.0528)

35. Zaffos A, Finnegan S, Peters SE. 2017 Plate tectonic regulation of global marine animal diversity. PNAS **114**, 5653-5658. (doi:10.1073/pnas.1702297114)

36. Buckley LB, Davies TJ, Ackerly DD, Kraft NJB, Harrison SP, Anacker BL, Cornell HV, Damschen EI, Grytnes J-A, Hawkins BA et al. 2010 Phylogeny, niche conservatism and the latitudinal diversity gradient in mammals. Proc. R. Soc. B **277**, 2131-2138. (doi: 10.1098/rspb.2010.0179)

37. Condamine FL, Sperling FAH, Wahlberg N, Rasplus J-Y, Kergoat GJ. 2012 What causes latitudinal gradients in species diversity? Evolutionary processes and ecological constraints on swallowtail biodiversity. Ecol. Lett. **15**, 267-277. (doi: 10.1111/j.1461-0248.2011.01737.x)

38. Jetz W, Fine PVA. 2012 Global gradients in vertebrate diversity predicted by historical area-productivity dynamics and contemporary environment. PLoS Biol. **10**, e1001292. (doi:10.1371/journal.pbio.1001292)

437   39. Pyron RA, Wiens JJ. 2013 Large-scale phylogenetic analyses reveal the causes of
438   high tropical amphibian diversity. Proc. R. Soc. B **280**, 20131622. (doi:
439   10.1098/rspb.2013.1622)

440   40. Parrish JT. 1993 Climate of the supercontinent Pangea. J. Geol. **101**, 215-233.
441   (doi:10.1086/648217)

442   41. Preto N, Kustatscher E, Wignall PB. 2010 Triassic climates – state of the art and
443   perspectives. Palaeo3 **290**, 1-10. (doi:10.1016/j.palaeo.2010.03.015)

444   42. Trotter JA, Williams IS, Nicora A, Mazza M, Rigo M. 2015 Long-term cycles of
445   Triassic climate change: a new $\delta^{18}O$ record from conodont apatite. Earth Plan. Sci.
446   Lett. **415**, 165-174. (doi: 10.1016/j.epsl.2015.01.038)

447   43. Wignall PB. 2015 The Worst of Times: How Life on Earth Survived Eighty Million
448   Years of Extinctions. Princeton University Press, 199p.

449   44. Sun Y, Joachimski MM, Wignall PB, Yan C, Chen Y, Jiang H, Wang L, Lai X. 2012
450   Lethally hot temperatures during the Early Triassic greenhouse. Science **338**, 366-
451   370. (doi:10.1126/science.1224126)

452   45. Penn JL, Deutsch C, Payne JL, Sperling EA. 2018 Temperature-dependent hypoxia
453   explains biogeography and severity of end-Permian marine mass extinction. Science
454   **362**, eaat1327. (doi:10.1126/science.aat1327)

455   46. Song H, Wignall PB, Dunhill AM. 2018 Decoupled taxonomic and ecological
456   recoveries from the Permo-Triassic extinction. Sci. Adv. **4**, eaat5091.
457   (doi:10.1126/sciadv.aat5091)

458   47. Smith RMH, Botha-Brink J. 2014 Anatomy of a mass extinction: sedimentological and
459   taphonomic evidence for drought-induced die-offs at the Permo-Triassic boundary in
460   the main Karoo Basin, South Africa. Palaeo3 **396**, 99-118.
461   (doi:10.1016/j.palaeo.2014.01.002)

462   48. Looy CV, Ranks SL, Chaney DS, Sanchez S, Steyer J-S, Smith RMH, Sidor CA,
463   Myers TS, Ide O, Tabor NJ. 2016 Biological and physical evidence for extreme
464   seasonality in central Permian Pangea. Palaeo3 **451**, 210-226.
465   (doi:10.1016/j.palaeo.2016.02.016)

466   49. Tabor NJ, Sidor CA, Smith RMH, Nesbitt SJ, Angielczyk KD. 2018 Paleosols of the
467   Permian-Triassic: proxies for rainfall, climate change, and major changes in
468   terrestrial tetrapod diversity. J. Vert. Paleo. **37(6)**, S240-253.
469   (doi:10.1080/02724634.2017.1415211)

470   50. Beerling DJ, Harfoot M, Lomax B, Pyle JA. 2007 The stability of the stratospheric
471   ozone layer during the end-Permian eruption of the Siberian Traps. Phil. Trans. R.
472   Soc. A **365**, 1843-1866. (doi:10.1098/rsta.2007.2046)

51. Benca JP, Duijnstee IAP, Looy CV. 2018 UV-B–induced forest sterility: implications of ozone shield failure in Earth's largest extinction. Sci. Adv. **4**, e1700618. (doi:10.1126/sciadv.1700618)

52. Bernardi M, Petti FM, Benton MJ. 2018 Tetrapod distribution and temperature rise during the Permian-Triassic mass extinction. Proc. R. Soc. B **285**, 20172331. (doi:10.1098/rspb.2017.2331)

53. Sidor CA, Vilhena DA, Angielczyk KD, Huttenlocker AK, Nesbitt SJ, Peecook BR, Steyer JS, Smith RMH, Tsuji LA. 2013 Provincialization of terrestrial faunas following the end-Permian mass extinction. PNAS **110**, 8129-8133. (doi:10.1073/pnas.1302323110)

54. Button DJ, Lloyd GT, Ezcurra MD, Butler RJ. 2017 Mass extinctions drove increased global faunal cosmopolitanism on the supercontinent Pangaea. Nat. Commun. **8**, 733. (doi:10.1038/s41467-01700827-7)

55. Ezcurra MD, Butler RJ. 2018 The rise of the ruling reptiles and ecosystem recovery from the Permo-Triassic mass extinction. Proc. R. Soc. B **285**, 20180361. (doi:10.1098/rspb.2018.0361)

56. Benson RBJ, Butler RJ. 2011 Uncovering the diversification history of marine tetrapods: ecology influences the effect of geological sampling biases. Geol. Soc. Lond., Spec. Pub. **358**, 191-208. (doi:10.1144/SP358.13)

57. Pörtner HO. 2002 Climate variations and the physiological basis of temperature dependent biogeography: systemic to molecular hierarchy of thermal tolerance in animals. Comp. Biochem. Physiol. A **132**, 739-761. (doi: 10.1016/S1095-6433(02)00045-4)

58. Brocklehurst N, Day MO, Rubidge BS, Fröbisch J. 2017 Olson's Extinction and the latitudinal biodiversity gradient of tetrapods in the Permian. Proc. R. Soc. B **284**, 20170231. (doi:10.1098/rspb.2017.0231)

59. Allen BJ, Wignall PB, Hill DJ, Saupe EE, Dunhill AM. 2020 Data from: The latitudinal diversity gradient of tetrapods across the Permo-Triassic mass extinction and recovery interval. Dryad. (doi:10.5061/dryad.m63xsj3zk)

60. Scotese CR. 2016 PALEOMAP PaleoAtlas for GPlates and the PaleoData Plotter Program. Version 2. PALEOMAP Project, http://www.earthbyte.org/paleomap-paleoatlas-for-gplates/

61. Müller RD, Cannon J, Qin X, Watson RJ, Gurnis M, Williams S, Pfaffelmoser T, Seton M, Russell SHJ, Zahirovic S. 2018 GPlates: building a virtual Earth through deep time. Geochem. Geophys. Geosyst. **19**, 2243-2261. (doi:10.1029/2018GC007584)

509   62. R Core Team. 2018 R: A language and environment for statistical computing.
510   Version 3.5.1. R Foundation for Statistical Computing, Vienna, Austria, https://www.r-
511   project.org/

512   63. Wickham H. 2017 tidyverse: Easily install and load the 'tidyverse'. Version 1.2.1.
513   https://cran.r-project.org/package=tidyverse

514   64. Alroy J. 2010 Geographical, environmental and intrinsic biotic controls on
515   Phanerozoic marine diversification. Palaeontology **53**, 1211-1235.
516   (doi:10.1111/j.1475-4983.2010.01011.x)

517   65. Benson RBJ, Butler RJ, Lindgren J, Smith AS. 2010 Mesozoic marine tetrapod
518   diversity: mass extinctions and temporal heterogeneity in geological megabiases
519   affecting vertebrates. Proc. R. Soc. B **277**, 829-834. (doi:10.1098/rspb.2009.1845)

520   66. Benton MJ, Dunhill AM, Lloyd GT, Marx FG. 2011 Assessing the quality of the fossil
521   record: insights from vertebrates. Geol. Soc. Lond., Spec. Pub. **358**, 63-94.
522   (doi:10.1144/SP358.6)

523   67. Benson RBJ, Upchurch P. 2013 Diversity trends in the establishment of terrestrial
524   vertebrate ecosystems: interactions between spatial and temporal sampling biases.
525   Geology **41**, 43-46. (doi:10.1130/G33543.1)

526   68. Vilhena DA, Smith AB. 2013 Spatial bias in the marine fossil record. PLoS ONE **8**,
527   e74470. (doi:10.1371/journal.pone.0074470)

528   69. Close RA, Benson RBJ, Upchurch P, Butler RJ. 2017 Controlling for the species-area
529   effect supports constrained long-term Mesozoic terrestrial vertebrate diversification.
530   Nat. Commun. **8**, 15381. (doi:10.1038/ncomms15381)

531   70. Darroch SA, Saupe EE. 2018 Reconstructing geographic range-size dynamics from
532   fossil data. Paleobiology **44**, 25-39. (doi:10.1017/pab.2017.25)

533   71. Fraser D. 2017 Can latitudinal richness gradients be measured in the terrestrial fossil
534   record? Paleobiology **43**, 479-494. (doi:10.1017/pab.2017.2)

535   72. Close RA, Evers SW, Alroy J, Butler RJ. 2018 How should we estimate diversity in
536   the fossil record? Testing richness estimators using sampling-standardised discovery
537   curves. Meth. Ecol. Evol. **9**, 1386-1400. (doi:10.1111/2041-210x.12987)

538   73. Alroy J. 2020 On four measures of taxonomic richness. Paleobiology in press.
539   (doi:10.1017/pab.2019.40)

540   74. Chao A, Jost L. 2012 Coverage-based rarefaction and extrapolation: standardizing
541   samples by completeness rather than size. Ecology **93**, 2533-2547. (doi:10.1890/11-
542   1952.1)

543   75. Hsieh TC, Ma KH, Chao A. 2016 iNEXT: an R package for rarefaction and
544   extrapolation of species diversity (Hill numbers). Meth. Ecol. Evol. **7**, 1451-1456.
545   (doi:10.1111/2041-210X.12613)

546   76. Alroy J. 2018 Limits to species richness in terrestrial communities. Ecology Letters
547   **21**, 1781-1789. (doi:10.1111/ele.13152)
548   77. Dunne EM, Close RA, Button DJ, Brocklehurst N, Cashmore DD, Lloyd GT, Butler
549   RJ. 2018 Diversity change during the rise of tetrapods and the impact of the
550   'Carboniferous rainforest collapse'. Proc. R. Soc. B **285**, 20172730.
551   (doi:10.1098/rspb.2017.2730)
552   78. Roscher M, Stordal F, Svensen H. 2011 The effect of global warming and global
553   cooling on the distribution of the latest Permian climate zones. Palaeo3 **309**, 186-
554   200. (doi:10.1016/j.palaeo.2011.05.042)
555   79. Krystyn L, Richoz S, Baud A, Twitchett RJ. 2003 A unique Permian-Triassic
556   boundary section from the Neotethyan Hawasina Basin, Central Oman Mountains.
557   Palaeo3 **191**, 329-344. (doi:10.1016/S0031-0182(02)00670-3)
558   80. Jalil N-E. 1999 Continental Permian and Triassic vertebrate localities from Algeria
559   and Morocco and their stratigraphical correlations. Jour. African Ear. Sci. **29**, 219-
560   226. (doi:10.1016/S0899-5362(99)00091-3)
561   81. Harris JM, Carroll RL. 1977 Kenyasaurus, a new eosuchian reptile from the Early
562   Triassic of Kenya. Jour. Palaeo. **51**, 139-149.
563   82. Shishkin MA, Novikov IV. 2017 Early stages of recovery of the East European
564   tetrapod fauna after the end-Permian crisis. Paleo. Jour. **51**, 612-622.
565   (doi:10.1134/S0031030117060089)